CHEMISTRY OF MATERIALS

ARTICLE

pubs.acs.org/cm

Encapsulation of *S. cerevisiae* in Poly(glycerol) Silicate Derived Matrices: Effect of Matrix Additives and Cell Metabolic Phase on Long-Term Viability and Rate of Gene Expression

Jason C. Harper,[†,§] DeAnna M. Lopez,[§] Elizabeth C. Larkin,[⊥] Megan K. Economides,[†] Sarah K. McIntyre,[§] Todd M. Alam,[§] Michaelann S. Tartis,[⊥] Margaret Werner-Washburne,[‡] C. Jeffrey Brinker,[*,†,‡,§] Susan M. Brozik,[*,†,§] and David R. Wheeler[*,§]

[†]Departments of Chemical and Nuclear Engineering and [‡]Molecular Genetics and Microbiology, University of New Mexico, Albuquerque, New Mexico 87131, United States

[⊥]Department of Chemical Engineering, New Mexico Institute of Mining and Technology, Socorro, New Mexico 87801, United States

[§]Sandia National Laboratories, Albuquerque, New Mexico 87106, United States

Supporting Information

ABSTRACT: Bioencapsulation of living cells into silica materials derived from the sol−gel process has resulted in novel hybrid living materials with exciting functionalities. Despite the many successes in this field, long-term viability and activity of the encapsulated cells remain a significant obstacle to producing practical and robust devices, e.g., whole-cell-based biosensors. We report the first study on the effects of various media additives and the metabolic phase of encapsulated cells on long-term viability and the rate of inducible gene expression. *Saccharomyces cerevisiae (S. cerevisiae)* cells, genetically engineered to produce yellow fluorescent protein (YFP) in response to galactose, were encapsulated in poly(glycerol) silicate derived matrices. Surprisingly, we find that addition of media components to the glycerol-silica matrix adversely impacted long-term viability in all cases studied, with a 1.3, 1.4, or 5.4 fold decrease in viability after only 9 days of storage in matrices containing yeast peptone dextrose (YPD), yeast peptone (YP, no glucose), or Synthetic Complete (SC) +2% glucose media, respectively. These findings are attributed to the media components inducing exit of the cells from the more robust quiescent state, and the metabolic production of toxic byproducts. Encapsulated cells from exponential culture exhibited inducible reporter gene expression rates approximately 33% higher than cells from stationary cultures. Addition of media components to the silica matrix increased gene expression rates under certain conditions. These results further elaborate on other silica matrix encapsulated living cell studies, and provide important design parameters for developing effective living cell-based biosensors for case-specific detection applications.

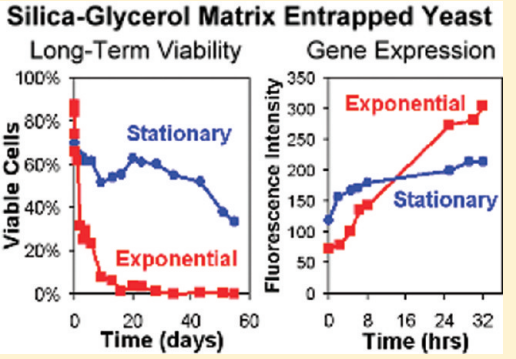

KEYWORDS: living hybrid biomaterials, bioencapsulation, glycerol modified silanes, cell viability, cell metabolic phase, whole-cell based biosensors

INTRODUCTION

The integration of living cells into silica matrixes by the sol−gel process continues to be a challenging field of research that offers many potential opportunities. Numerous researchers have reported the generation of novel hybrid living materials that confer protection to the encapsulated cells, enhance long-term viability, and provide control over bio/nano interfacial properties and the environment local to the cells.[1−7] Such control can provide an instructive background needed to achieve specific functionalities and guide cellular behavior.[8−12] Hybrid living materials with these properties can enable significant advances in biotechnological applications including biosensing, biocatalysis, tissue/organ replacement, environmental and industrial process monitoring, controlled delivery of therapeutics, and bioelectronics.[13−15]

Silica materials derived from sol−gel processing have several differentiating advantages over other polymers used for cellular encapsulation. These include the ability to retain water with negligible swelling, chemical and biological inertness, mechanical stability, controlled porosity, resistance to microbial attack, room-temperature preparation, optical transparency, and the ease with which the chemistry of the sol−gel can be varied.[16−18] Indeed, silica is an archetypical cell-protectant in nature. Diatoms, radiolarians, and sponges have evolved to fix silica onto their cell surfaces, forming exoskeletons that can provide mechanical protection without adversely effecting nutrient and waste exchange required for growth.[19]

The high chemical and biological stability and excellent transparency inherent to sol−gel derived silica materials has been leveraged to produce effective silica matrix entrapped whole

Received: December 11, 2010
Revised: March 28, 2011
Published: April 27, 2011

cell-based biosensors. In these devices, the intact living cell serves as the active element, exploiting the intrinsic ability of cells to sense their environment and respond to various molecules and stresses. Cell responses are tunable, typically using genetic engineering and signal amplification approaches to produce a detectable signal. For example, Premkumar et al.[20,21] encapsulated *Escherichia coli* (*E. coli*) strains engineered to respond to general toxicity, genotoxicity, and oxidative stress, in tetramethylorthosilicate (TMOS) derived silicate films. Exposure to various toxins was monitored by production of an exogenous bioluminescence. Production of fluorescent proteins by silica entrapped *E. coli* has also been employed for sensing,[22] and a careful study of the advantages/disadvantages of both luminescent and fluorescent systems has been reported.[23] Silica entrapped living cell-based sensors for biochemical oxygen demand (BOD),[24] naphthalene and salicylate,[25] antiphoto system II herbicides,[26] organophosphates,[27] dicyclopropyl ketone,[28] and other physiological stresses[29,30] have been reported.

Despite these many successes, long-term viability and activity remains a significant obstacle in producing practical and robust living cell-based biosensors. It was recently suggested that adding nutrients to a glycerol-containing silica matrix may improve long-term cellular viability.[31] Additionally, the metabolic state of the cell upon encapsulation may also hold importance in viability and sensing activity. Cells from stationary phase cultures are known to be more resistant to stresses that may occur upon encapsulation, whereas cells from exponential phase cultures are more responsive by way of inducible reporter gene expression,[32] both being vital for effective sensing. A survey of the literature shows that although cells from both exponential and stationary phase cultures are encapsulated for sensing applications, the impact of cell metabolic state on long-term viability and sensor activity has not been addressed.

Herein, we present what we believe to be the first study investigating the effects of media additives and metabolic phase of silica matrix encapsulated yeast cells on long-term viability and the rate of inducible gene expression. *Saccharomyces cerevisiae* (*S. cerevisiae*), genetically engineered to produce yellow fluorescent protein (YFP) in response to galactose, which serves as a model analyte for sensing applications, was encapsulated in a sol−gel matrix derived from the hydrolysis of a glycerol orthosilicate with media, in which the presence of fermentable carbon and other nutrients was independently varied. Interestingly, we observed that in all cases, *S. cerevisiae* viability was negatively impacted by the presence of a fermentable carbon source, and/or other nutrients in the silica matrix. The presence of nutrients and fermentable carbon had a positive or negative effect on the rate of inducible gene expression that was dependent on the cell metabolic phase and encapsulation time in the silica matrix. Encapsulated cells from exponential phase cultures showed enhanced inducible gene expression while cells from stationary phase cultures showed significantly greater long-term viability. These insights provide valuable design parameters that may facilitate the development of robust and effective silica encapsulated whole-cell based sensors for case-specific applications such as online process monitoring or autonomous environmental sensing.

EXPERIMENTAL SECTION

Materials. Aqueous solutions were prepared with 18 MΩ water using a Barnstead Nanopure water purifier (Boston, MA). Tetraethylorthosilicate (TEOS), glycerol (anhydrous), glucose (99%), galactose (99%), and titanium isopropoxide (97%) were purchased from Sigma-Aldrich (St. Louis, MO). Phosphate buffer saline (PBS) solution, pH 7.2 (11.9 mM phosphates, 137 mM NaCl, and 2.7 mM KCl at 1× concentration), hydrochloric acid (HCl), sodium hydroxide (NaOH), sodium phosphate (monobasic and dibasic), and yeast extract were obtained from Fischer Scientific (Pittsburgh, PA). Bacto Peptone was from BD Biosciences (Franklin Lakes, NJ). Yeast nitrogen base (YNB) w/o amino acids was from Formedium, LTD (Hunstanton, England), and Drop-out Mix Complete (w/o YNB) was from U.S. Biological (Swampscott, MA). *Funga* Light CFDA/PI yeast viability kit was purchased from Invitrogen (Carlsbad, CA). All reagents were used as received.

Yeast Culture Mediums. Yeast extract, peptone, dextrose (YPD) media contained 10 g of yeast extract, 20 g of Bacto peptone, and 20 g of glucose per 1 L of nanopure water. For YPD-agar plates, 20 g of agar was added to YPD media. In yeast extract, peptone, galactose (YP + gal) induction medium, the 20 g of glucose in the YPD recipe was replaced with 20 g of galactose. YP media was identical to YPD media without addition of glucose. Synthetic complete with glucose (SC + 2% glu) contained 5.9 g of YNB w/o amino acids, 550 mg KCl, 2 g of Drop-out Mix Complete, and 20 g of glucose per 1 L of nanopure water.

Synthesis of Poly(glycerol) Silicate.[33] A round-bottomed flask equipped with a stir bar, dropping funnel, and reflux condenser was charged with 63.4 g of glycerol (688 mmol) and heated to 60 °C with stirring. To the hot glycerol was added a mixture of 10.21 g TEOS (49.0 mmol) and 1.02 g of titanium isopropoxide (3.0 mmol). After addition, the reaction mixture was refluxed at 130 °C for 3 h. Ethanol coproduct was removed under vacuum (∼10 mTorr) at 130 °C. The product (63.5 g; 98% yield) was a viscose opalescent white liquid that was somewhat soluble with water. The mass of the product agreed with the reported theoretical formula: $Si(C_3H_7O_3)_4 \cdot 10C_3H_8O_3$;[33] however, it is certain that many isomers exist in the mixture as well as some inadvertent hydrolysis products.

Preparation of Poly(glycerol) Silicate (PGS) Derived Silica Gels and Encapsulated *S. cerevisiae* Monoliths. For gelation time point experiments, a given volume percent (20, 35, 50, 65, 80%) of buffer or media was added to the PGS (3 mL total volume) in a polystyrene 15 mL centrifuge tube and homogenized by vortexing for 60 s. For silica matrix encapsulated *S. cerevisiae* monoliths, 50 volume percent of *S. cerevisiae* cells (1×10^6 to 1×10^7 cells/mL) in a given media or buffer previously adjusted to pH 6.0, was added to the PGS (250−350 μL total volume) in a 1.5 mL polypropylene microcentrifuge tube and homogenized by vortexing for 60 s. All samples were allowed to gel in the centrifuge tubes and stored capped at room temperature (22 °C). The theoretical density of the final wet gels corresponds to 1.1−1.3 g cm^{-3}.

Fluorescence and SEM Imaging. Fluorescence microscopy imaging was performed on an Olympus IX70 microscope and recorded using an Olympus DP71 camera. A Hitachi 3200N scanning electron microscope (SEM) operating at 25 kV was used to directly image poly(glycerol) silica gel encapsulated *S. cerevisiae* cells on a graphite support ∼6 h post gelation, without further preparation.

^{29}Si NMR Analysis. ^{29}Si solution state NMR spectra of the PGS were obtained on a Bruker DRX 400 using a 10 mm ^{29}Si-selective probe. The ^{1}H-decoupled ^{29}Si spectra were acquired using an inverse gating pulse sequence with 512 scans and a 60 s recycle delay. The spectra were referenced to the external secondary standard of neat TMS at $\delta(^{29}Si) = 0$ ppm. The solid state ^{29}Si magic angle spinning (MAS) NMR spectra of silica-glycerol gels were obtained on a Bruker Avance 400 using a 7 mm broadband probe spinning at 4 kHz, with 4k scans and a 240 s recycle delay using a standard single pulse Bloch decay sequence. The solid state spectra were referenced to the secondary external standard Q_8M_8 at $\delta(^{29}Si)$ = 11.8 ppm with respect to TMS. The degree of

condensation (C) was defined based on the relative concentrations of the different Q^n species:

$$C = \frac{[Q^1] + 2[Q^2] + 3[Q^3] + 4[Q^4]}{4}$$

Long-Term Viability Measurements. Encapsulated *S. cerevisiae* cell viability was measured using three methods: fluorescence dyes, 24 h culture in YDP medium, and 48 h growth on YPD-agar. For viability dye assays, the *Funga* Light assay was used, which contains a cell-permeable nonspecific esterase substrate (CFDA) and a cell membrane integrity indicator (PI). Viability assay was performed using the manufacturer's protocol with slight modifications: 1 μL of CFDA solution (1 mg in 100 μL of DMSO) and 1 μL of PI solution (20 mM in H_2O) was added to 1 mL of 1× PBS, pH 7.4. From this solution, 250 μL was pipetted on top of a glycerol−silica gel encapsulated *S. cerevisiae* cell monolith and incubated for 45−60 min at 30 °C. Following incubation a portion of the monolith was removed from the microcentrifuge tube by scrapping the monolith with a small sterile wooden dowel. This portion was then mounted between a glass microscope slide and coverslip. Cells were then imaged with an inverted fluorescence microscope. Cells with esterase activity and intact membranes fluoresced green and were counted as viable. Cells without esterase activity and damaged membranes fluoresced red, cells with residual esterase activity and damaged membranes fluoresced yellow, and neither was counted as viable.

As viability is ultimately defined as the ability of a cell to reproduce, cell culture and the ability of cells to form colonies on solid medium plates was also used to assess viability. For 24 h culture, a portion of a glycerol−silica gel encapsulated *S. cerevisiae* cell monolith was removed and mixed with 200 μL of 1× PBS, pH 7.4, forming a homogeneous suspension. From this cell−PBS suspension, 100 μL was added to 5 mL of YPD medium in a 15 mL culture tube from which 100 μL was retained for the 48 h growth on YDP-agar plates (described below). The remainder was incubated with shaking at 30 °C for 24 h. The optical density at 600 nm ($O.D._{600}$) was measured at time = 0 and 24 h using a μQuant microplate reader (Bio-Tek Instruments, Winooski, VT). For the 48 h growth on YDP-agar plates, the retained 100 μL cell-YPD suspension was spread onto YPD-agar in a plastic 10 cm Petri dish and incubated at 30 °C for 48 h.

Rate of Inducible Gene Expression Measurements. The rate of gene expression was monitored by measuring the fluorescence intensity with time of the reporter protein, yellow fluorescent protein (YFP). For induction of YFP expression in *S. cerevisiae* culture, exponential or stationary phase cells were pelletted by centrifugation and resuspended in YP +gal induction medium. The cells were incubated with shaking, or under stagnant conditions, at 30 °C. At given time intervals, a 50−100 μL aliquot was removed from the culture, pelleted, aspirated, and resuspended in 1× PBS, pH 7.4. Cells were imaged via fluorescence microscopy. For PGS derived sol−gel matrix encapsulated *S. cerevisiae* cells 250 μL of YP +gal was pipetted on top of the matrix, followed by incubation at 30 °C for various times between 0 and 32 h. A separate monolith was prepared for each time point. Following the incubation, a portion of the monolith was removed, mounted between a glass microscope slide and coverslip, and imaged. Identical microscope and camera settings were used for all imaging allowing quantitative analysis of YFP expression between all samples imaged. The limit of fluorescence detection represents the lowest fluorescence intensity of a positive control whose signal strength is greater than the sum of the mean fluorescent intensity of a negative control sample (μ) and its standard deviation (σ) multiplied by 3 ($LOD_{Fluor.} = \mu + 3\sigma$). The time required for a given sample to develop a fluorescence intensity greater than the LOD_{Fluor} was used to compare the rate of YFP expression between samples.

RESULTS AND DISCUSSION

Poly(glycerol) Silicate (PGS) Synthesis and Characterization. Increasing interest has developed in use of alkoxysilanes modified with diols or polyols for cellular encapsulation due to the attractive properties of these systems including high water solubility (no organic cosolvent required), initiation of hydrolysis and condensation reactions by the addition of water (no requirement of acid or base catalyst), and hydrolysis products that are biocompatible alcohols. Several diol or polyol modified silicates have been reported utilizing ethylene glycol, propane-1,2-diol, or glycerol.[34−36] In studies where diol/polyol-modified alkoxysilanes have been used for cellular encapsulation, or in which diols/polyols have been added directly to a silica matrix used for cellular encapsulation, glycerol provided the greatest enhancement in cellular viability.[37,38] This is attributed to the high osmolarity of glycerol, which decreases the activity of water, and can be transported through the cell membrane via aquaglyceroporins, modifying the membrane permeability.[39] Therefore, a recently reported PGS was selected for use in this study that, to the best of our knowledge, has not yet been used for encapsulation of cells.

The starting material for the synthesis of the glycerol derived silicate was similar to that by Khonina et al.[33] with the catalyst substitution of titanium isopropoxide for titanium butoxide and a 10:1 molar ratio of glycerol to tetraethylorthosilicate (TEOS). One can expect a variety of different isomers to be present including cyclics and potential dimers and other oligiomers. No attempt was made to characterize the exact species present or their ratios. Slight variations in batches as evidenced by different gelation times (±10%) can reasonably be attributed to variations in the ratios of species present. Despite attempts to maintain tight control of reactions conditions, these variations likely arise from slight difference in reaction temperature, and additions rates, as well as slight variations in the amount of adventitious water present. We believe that the overall gelation process is not affected to a large extent by these slight variations, and no sensitivity of the entrapped cells to these variations was observed.

The hydrolytic stability of the synthesized PGS was investigated by ^{29}Si solution NMR. Multiple resonances were observed indicating that multiple Q^0 hydrolyzed species exist (major peaks at −82, −83, −84, and −85 ppm and minor Q^1 condensation peaks at −89, −90, and −91 ppm;[40,41] spectrum presented in the Supporting Information, Figure S1). The degree of condensation of the as synthesized material after 2 months of capped storage at room temperature was 5%. This low degree of condensation is indicative of the relatively high hydrolytic stability of this material when compared to similar materials prepared from alternative methods.[34,42] Silica gels formed from PGS stocks more than 6 months old exhibited negligible variation in gelation time, mechanical, and optical properties.

Gel Formation. The gelation characteristics of this material as a function of pH, theoretical SiO_2 weight percent, and in the presence of various yeast culture media are presented in Figure 1. Gelation time was defined as the point at which the aqueous buffer-PGS mixture no longer flowed when inverted. Of the ±10% batch to batch gelation time variation, 1−2% is attributed to the somewhat subjective determination of zero flow. An increase in gelation time as the pH decreased, with a sharp increase between pH 2−4, was observed (Figure 1A). This pH range corresponds to the isoelectric and zero charge points of silica and common tetraalkoxysilanes,[43] where silica

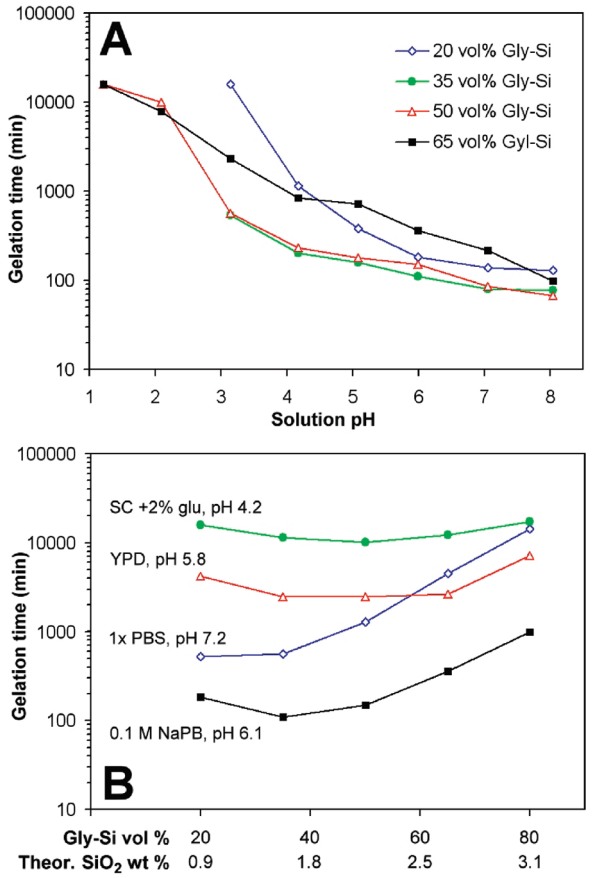

Figure 1. (A) Gelation time following introduction of 20, 35, 50, or 65 vol % PGS into buffered solutions at pH 1.21, 2.09, 3.14, 4.17, 5.08, 5.99, 7.05, or 8.05. (B) Gelation time following introduction of 20, 35, 50, 65 or 80 vol % PGS into SC +2% glu, YPD, 1× PBS, or 0.1 M NaPB solutions.

Table 1. Solid-State ^{29}Si MAS NMR Spectral Data for PGS-Derived Silica Gels with and without Entrapped Yeast[a]

	$\delta(^{29}\text{Si})$ (ppm)	relative integration (%)
sol−gel only	−111 Q^4	52
	−101 Q^3	48
sol−gel with entrapped yeast	−111 Q^4	59
	−102 Q^3	35
	−90.8 Q^2	6

[a] PGS-derived gels prepared with 50 vol % 0.1 M NaPB, pH 6.0. Spectra collected approximately 25 days post gelation.

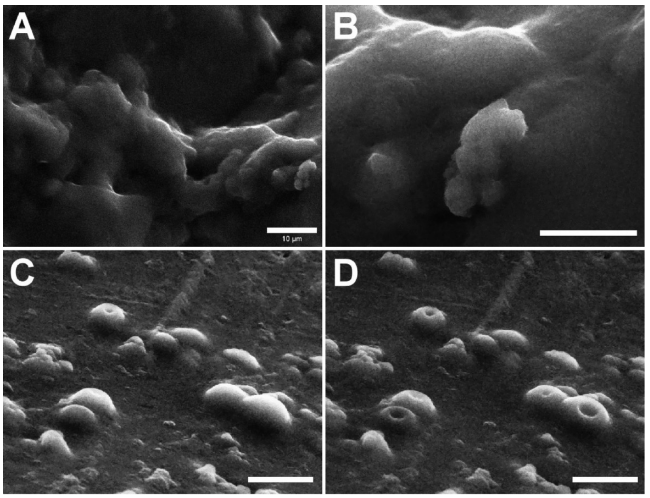

Figure 2. SEM images of PGS derived silica gels containing *S. cerevisiae* cells. (A) Typical long-range morphology with some shallowly encapsulated cells visible (B). Image (D) was collected several minutes after image (C), showing development of depressions during imaging. Scale bars in (B−D) are 5 μm.

condensation kinetics are minimized, resulting in longer gelation times. This observation corresponds well with trends observed in other glycol-based systems.[34] The effect of theoretical SiO_2 weight percent on gelation time was also studied by increasing or decreasing the volume percent of the PGS in the silicate-aqueous buffer mixture. As shown in Figures 1A and B, a minimum in gelation time is generally observed between 1.6 and 2.1 theoretical SiO_2 weight percent (35−50 vol% PGS in 0.1 M sodium phosphate, NaPB). Below this range, the increase in gelation time is attributed to the low concentration of silica in the mixture. The resulting gels also exhibited decreased mechanical integrity (data not shown). Above this range, the increase in gelation time is attributed to the lower relative concentration of the H_2O catalyst.

The incorporation of yeast culture media, as a general trend, increased gelation time of the PGS as pH decreased (Figure 1B) with a minimum gelation time, again near 1.6−2.1 theoretical SiO_2 weight percent. An exception to these trends is the gelation time of 1× PBS (pH 7.2). Based on the pH trends observed in Figure 1A and the higher ionic concentration of this solution (~0.152 M), it may be expected that 1× PBS would yield similar, if not shorter gelation times than 0.1 M NaPB (pH 6.1). Although the hydrolysis and condensation reactions for common tetraalkoxylsilanes are well understood, little is known regarding the hydrolysis and condensation behavior of glycol modified silianes.[34] This is further complicated by conflicting reports on the impact, or lack thereof, of ionic strength and pH on the gelation of various poly(glycerol) silicate derived sol−gels.[34,44] On the basis of the results shown in Figure 1, encapsulated cell monoliths were prepared by mixing a 1:1 volume ratio (2.1 theoretical SiO_2 wt %; 50 vol %) of the PGS, with the given medium, pH adjusted to 6.0. This provided a silica gel at a pH amenable to cellular viability, sufficient mechanical integrity, and practical gelation times.

Gel Structural Characterization. The degree of silica condensation for PGS derived gels, with and without cells, was measured using solid state ^{29}Si MAS NMR. Table 1 contains the ^{29}Si NMR spectral data from monoliths formed from 50 vol% PGS in 0.1 M NaPB, pH 6.0, and allowed to age for approximately 25 days. From this data, the degree of condensation (C) for monoliths without *S. cerevisiae* cells, and with *S. cerevisiae* cells, was calculated to be 88.1% and 88.2%, respectively. These results show that although a substantial degree of silica has condensed, condensation was not complete. Furthermore, the chemistry of the sol−gel system was not extensively changed by the presence of *S. cerevisiae* cells at the concentrations used. Unfortunately, the initial kinetics of the gelation reaction are too fast to accurately observe via ^{29}Si NMR given the long recycle delay required for complete relaxation and large dilution of the silica upon addition of the buffer or buffer/cell suspension. Within eight minutes of mixing, the Q^0 sites of the original material had decreased to 10%

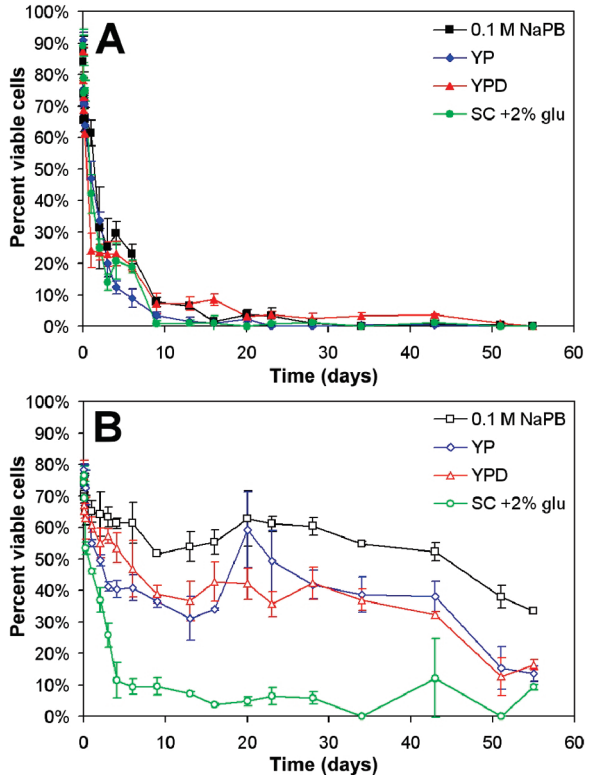

Figure 3. Viability of *S. cerevisiae* cells from (A) exponential culture and (B) stationary culture encapsulated in glycerol−silica gels derived from 50 vol % PGS and 50 vol % medium that was: nutrient- and fermentable-carbon-rich (YPD, red), nutrient-rich without fermentable carbon (YP, blue), nutrient-restricted and fermentable-carbon-rich (SC + 2% glu), or without nutrients or fermentable carbon (0.1 M NaPB, black). All mediums were adjusted to pH 6.0. Encapsulated cells stored at room temperature. Viability determined via CFDA/PI assay. Error bars are the standard deviation of measurements from 3 regions of a given sample.

of their initial intensity, and the very broad condensation Q^1 and Q^2 resonances were visible at low intensities. The initial spectrum of the PGS, and spectra acquired after addition of the buffer solution or buffer solution containing cells, are presented in Figures S2 and S3 in the Supporting Information.

The surface morphology of PGS derived gels containing *S. cerevisiae* cells was examined using scanning electron microscopy (SEM). SEM imaging was performed directly (without fixation, supercritical drying, or metal sputtering) on glycerol−silica gel monoliths. Figure 2A shows that the typical long-range morphology of glycerol−silica gels is globular, with some regions of disordered porosity visible. Shallowly encapsulated yeast cells are also visible, as shown by the higher magnification image of a small cluster of yeast cells (Figure 2B). These images suggest that the glycerol−silica matrix is not completely homogeneous. EDS measurements did not provide any evidence that the globular regions were high in salt or glycerol content; however, phase separation is known to occur in glycerol containing silica matrixes.[34] The formation of a high glycerol and water containing region surrounding cells entrapped in silica matrices has been reported, and that interface has been implicated in improved cellular viability.[31,37] Planar, less-globular surface regions are less frequently observed (Figure 2C). Depressions are also visible in many areas of the sample, and were observed to form as the sample was exposed to the electron beam (compare Figure 2C and 2D, imaging separated by a few minutes). These depressions are likely the result of the collapsing of silica matrix encapsulated yeast cells, as the cytosolic fluid evaporates because of local heating from the electron beam.

Effect of Cell Metabolic Phase and Media Additives on Long-Term Viability. The long-term viability of glycerol-silica gel encapsulated *S. cerevisiae* cells was explored with cell metabolic phase upon encapsulation, and various media component additives to the glycerol−silica matrix, as variables. For cell metabolic phase samples, *S. cerevisiae* cells from exponential phase culture (overnight cultures) and stationary phase culture (8 day old cultures) were used. Cells from these two cultures have significantly different metabolic properties. Cells in exponential phase culture derive their energy from aerobic fermentation, metabolizing carbon rich glucose via glycolysis, whereas cells in stationary phase culture have negligible energy requirement. The progression from exponential phase to stationary phase requires two metabolic shifts. Rapidly proliferating cells in exponential culture deplete fermentable carbon and undergo slow carbon starvation. The diauxic shift occurs when the cells change their metabolism to consume ethanol and nonfermentable carbon produced as byproducts of fermentation. A second metabolic shift occurs after all fermentation byproduct carbon is depleted and the cells readjust their metabolism, entering a maintenance-like resting state (quiescence), in which proliferation does not occur and the cells can remain viable without nutrients.[45]

In media additive experiments, the long-term viability of *S. cerevisiae* cells from exponential or stationary phase cultures encapsulated in PGS derived silica matrices containing a fermentable carbon source or other nutrients was studied. Four medium additives were used: a nutrient- and fermentable-carbon-rich media (YPD), a nutrient-rich media without fermentable carbon (YP), a nutrient-restricted and fermentable-carbon-rich media (SC +2% glucose), and simple buffer without nutrients or fermentable carbon (0.1 M NaPB). Figure 3A plots the viability of *S. cerevisiae* from exponential phase culture over 56 days of encapsulation in glycerol-silica matrix with various medium. Prior to gelation, cells in PGS-buffer/medium solution and cells from exponential phase culture had similar viabilities measured as 89 ± 2%. Following gelation (~2 h for all samples) viability dropped to 66 ± 6%. This loss in viability is attributed to the stresses exerted on the cells during the silica condensation reactions and the ensuing compressive stresses from gelation. Three regions of differing slope in viability are observed following gelation. The first region occurs over the first 2 days after gelation in which a rapid decline in viability is measured for cells encapsulated in all 4 mediums, resulting in viability between 23 and 34% after 2 days. This significant loss in viability may correspond to the lower concentration and decreased rate of diffusion of fermentable carbon and/or nutrients through the matrix leading to rapid death for these cells with high metabolic activity. The second region occurs between 2 and 9 days following gelation. Over this period the viability continues to drop, but at a decreased rate with some minor distinction between cells encapsulated in the 4 mediums. This region may correspond to a small population of cells that could enter the diauxic shift. However, by 9 days post gelation, viability for all samples decreased to less than 8%. This suggests that the effective concentration of metabolizable carbon was not high enough to permit the slow shift of metabolism from exponential growth, through nonfermentable carbon metabolism, to quiescence.

Finally, a third region extending from day 10 to 55 shows little change in viability with all data points between 0 and 7% viability.

For encapsulated cells from stationary culture (Figure 3B), a decrease in viability post gelation to 64 ± 8%, similar to cells from exponential culture, was measured and attributed to stresses exerted on the cells during gelation. However, viability following gelation was substantially improved. Three regions of differing slope were observed, which are similar between samples with different matrix additives. The first region spanned 1−9 days postgelation in which the greatest decline in viability was observed. The second region spanned approximately days 9 to 43. Viability in this region was, within experimental error, constant. In the fourth region, 43+ days after gelation, viability declined.

The viability of cells from stationary phase culture in the last three regions depended strongly on the nutrient and fermentable carbon source content of the encapsulation matrix. In control samples, *S. cerevisiae* cells were encapsulated in a glycerol-silica matrix with simple buffer (Figure 3B, black). Viability measured for these cells decreased to 51−61% over the first 1−9 day region. As the matrix lacked both nutrients and fermentable carbon, quiescent cells should remain in that state. We therefore propose that this loss in viability was due to residual syneresis exerting minor compressive stresses that damaged some cells. Additionally, a small population of cells may not have been adequately insulated from the polar chemical groups at the silica surface (i.e., silanols) by the glycerol, slowly leading to damage at the cell/gel interface, inducing cell lysis.[31] From 9 to 43 days following gelation, control cells viability remained nearly constant between 52 and 63%. This is slightly higher than the 40−50% viability 1 month post encapsulation that is commonly reported for glycerol containing films. Here, higher viabilities maybe due to the greater glycerol and lower Si content of these gels, and ensuring the *S. cerevisiae* cells were in stationary phase prior to encapsulation by culturing for 8 days, or a combination of these factors. Typically, postdiauxic shift cultures (∼2−4 days from inoculation) are used for encapsulation studies and incorrectly assumed to be in the stationary phase,[45] which may lead to differences from the data reported in this study. Also of note is the similarity of this measured viability to the recently reported 40−50% percent of yeast cells in a stationary phase culture that are truly quiescent, termed 'daughter cells'.[32] These cells are distinct from the remaining nonquiescent "mother cells". Finally, a drop in viability was observed 43 days following gelation. This loss in viability may be due to break down of the gel resulting in cell damaging compressive stresses, or exposure of the cell wall to damaging polar groups. Minor expulsion of fluid was observed in some monoliths prepared for the gelation time studies (Figure 1) 2−3 months after gelation.

For cells from stationary phase culture encapsulated in PGS derived silica matrices containing nutrient and fermentable carbon rich YPD media (Figure 3B, red), viability initially decreased from 62% to ∼40% over the first 9 days postgelation. We propose that this greater decrease in viability, compared to the control sample (black), is due to the quiescent cells sensing the presence of glucose, leading to exit of a subpopulation of the cells from quiescence.[46] However, the relatively low concentration and finite source of glucose is rapidly depleted. These cells may then enter diauxic shift and metabolize the nonfermentable carbon byproducts of fermentation. As the measured viability 9 to 43 days following gelation was between 32 and 43%, it is evident that addition of this complex media to the matrix resulted in a substantial loss in viability over the control sample. Cells encapsulated with nutrient rich medium without fermentable carbon (YP, Figure 3B, blue) showed nearly identical viability trends as YPD medium. One exception is the greater rate in loss of viability over the first 9 days following gelation. Like cells exposed to YPD (red), a portion of these cells from stationary phase culture may sense the presence of nutrients in the YP medium and exit quiescence. Glucose in water, in the absence of any other nutrients, is known to induce exit from quiescence.[46] However, it is unknown whether a few key nutrients or other chemical factors that may be present in the yeast extract or peptone can also induce exit from quiescence.[45] Still, as no fermentable carbon source is present, cells that exit quiescence ultimately die. Furthermore, as carbon fermentation was not possible, nonfermentable carbon byproducts cannot be present, reducing the likelihood of an effective diauxic shift. Hence the lower viability for these cells between days 1−9, as compared to cells encapsulated with YPD. Still, it would appear that nearly the same population of cells was lost for samples prepared with YP or YPD, indicating that the populations of cells that exit quiescence ultimately cannot return to a quiescent state and die regardless of the presence of a fermentable carbon source.

For nutrient-restricted and carbon-rich SC +2% glucose media (Figure 3B, green) cell viability rapidly decreased to 11 ± 6% after only 4 days. This loss in viability is much greater than that measured for cells encapsulated with YPD which contained the same concentration of glucose. Although SC media is commonly used in yeast cell culture, it was recently reported that yeast metabolism of SC media leads to formation of an undesirable byproduct, acetic acid, which can negatively impact viability.[47] Under shaken culture conditions, the produced acetic acid is quickly dispersed throughout the culture media, resulting in concentrations that are only moderately detrimental to the yeast cells. However, for silica matrix encapsulated yeast, the effective diffusion rate for the produced acetic acid is lower than under shaken culture conditions. This results in the development of an acetic acid concentration gradient, with high acetic acid concentrations within close proximity to the cells, leading to a substantial loss in viability. Additionally, the resultant pH gradient could detrimentally affect the surrounding silica matrix causing the cells to sustain additional stresses.

The fluorescence dye viability results (Figure 3) were also confirmed by freeing cells from the silica matrix followed by shaken culture and plating on solid medium. These results are presented in Table 2. Trends in cell viability observed from the culture and plating results were similar to those measured by fluorescence viability dye assay. (Images of colony growth on plates of previously entrapped *S. cerevisiae* cells from exponential and stationary cultures are presented in the Supporting Information, Figures S4 and S5, respectively). These results also demonstrate that encapsulated cells, when removed from the glycerol−silica matrix, remain viable and culturable.

Surprising, and contrary to what was predicted,[31] in all cases in which media components were added to the matrix, the viability of encapsulated *S. cerevisiae* cells was negatively impacted. This can be rationalized by comparing the viability data for cells from exponential versus stationary culture. For effective long-term viability, *S. cerevisiae* cells should be in the more robust quiescent state. Addition of media induces exit from quiescence and should be avoided to maintain long-term viability. A similar conclusion was drawn by Nassif et al. who showed substantially improved

Table 2. Reproductive Capability of *S. cerevisiae* Removed from Glycerol−Silica Gels with 50 vol % Medium Additives[a]

		24 h culture in YPD[c]				48 h incubation on YPD-Agar[d]			
		time stored[b] (weeks)							
		2	4	6	8	2	4	6	8
exponential	0.1 M NaPB	M	X	X	X	L	X	X	X
	YP	H	X	X	X	L	X	X	X
	YPD	L	L	L	X	M	L	L	X
	SC +2% glu	M	L	M	X	L	L	L	X
stationary	0.1 M NaPB	M	H	H	M	H	M	M	M
	YP	M	H	H	L	M	M	L	L
	YPD	H	M	H	M	H	M	H	H
	SC +2% glu	M	H	H	L	L	M	M	L

[a] All mediums were adjusted to pH 6.0. [b] Encapsulated cells stored at room temperature. [c] Optical density (OD) of cultures: high (H; $O.D._{600}$ = 1.6−3.0), moderate (M; $O.D._{600}$ = 1.1−1.5), low (L; $O.D._{600}$ = 0.6−1.0), and none (X; $O.D._{600}$ = 0.0−0.5). Measured values for each sample are reported in the Supporting Information (Table S1). [d] Relative number of CFUs: high (H), moderate (M), low (L), and none (X). Images of each sample are provided in the Supporting Information (Figures S4 and S5).

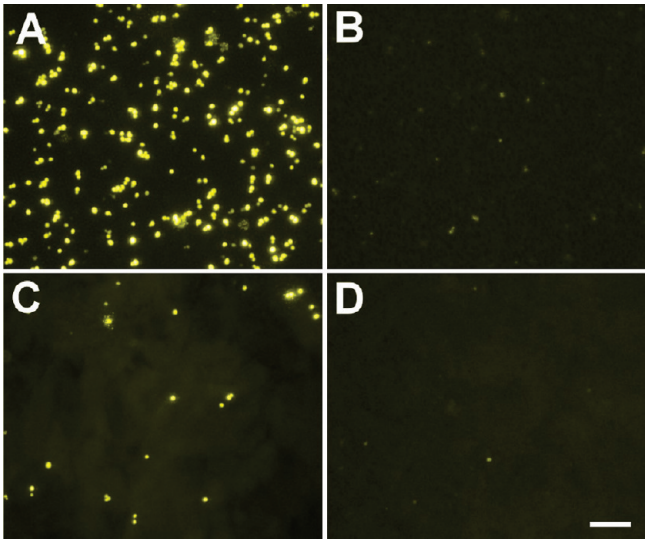

Figure 4. Fluorescence microscopy images (false colored) of (A, B) YFP expressing *S. cerevisiae* cells in exponential shaken culture, and (C, D) cells from exponential culture entrapped in a 1:1 (vol.) matrix of PGS: 0.1 M NaPB, pH 6.0, for 24 h. YFP expression was induced (YP +gal treatment overnight at 30 °C) in A and C. Control uninduced samples (YPD treatment overnight at 30 °C) are shown in B and D. Cell density in (C, D) silica matrix samples was approximately 25% the density in (A, B) culture samples. All images were captured under identical camera settings. Scale bar = 30 μm.

viability for glycerol−silica gel entrapped bacteria following addition of quorum sensing inducer molecules.[48] The authors suggest that these molecules maintain the bacteria in a stationary phase, enhancing their resistance to encapsulation-induced stresses.

Inducible Gene Expression. In addition to long-term viability, effective whole-cell based biosensors must recognize a particular analyte and then generate a measurable signal. This is typically done by genetically engineering cells to introduce an exogenous reporter protein that produces a fluorescence, luminescent, or electrochemical signal. Expression of this protein is controlled by selecting a promoter that is induced by either the target analyte itself, or a molecule that is produced as part of a cell signaling pathway activated by the target analyte.[49]

In this work, *S. cerevisiae* cells were engineered to produce yellow fluorescent protein (YFP) in the presence of the model analyte, galactose. The selectivity of this engineered stain for galactose over the monosaccharide epimer, glucose, is shown in Figure 4. Bright fluorescence was observed for engineered cells treated in shaken culture with YP +gal induction medium (Figure 4A), and for glycerol−silica encapsulated cells treated with YP +gal placed on top of the monoliths (Figure 4C). Engineered cells in shaken culture with YPD medium (Figure 4B), and silica matrix encapsulated cells treated with YPD (Figure 4D) showed very little background fluorescence. This dim fluorescence is often attributed to 'leaky promoter' expression of the recombinant protein. These results show the exceptional selectivity possible with cell-based biosensors. Additionally, fluorescence was observed from cells encapsulated deep within the silica monolith demonstrating that galactose and oxygen can diffuse throughout the glycerol−silica matrix.

Effect of Cell Metabolic Phase and Media Additives on Inducible Gene Expression. As fluorescence intensity from fluorescent proteins is a function of protein concentration, monitoring intensity over time provides information regarding the rate of expression of the protein. In addition to providing insights into cellular metabolism, the rate of reporter gene expression is also the governing parameter for response time of the cell-based sensor.

The rate of galactose-induced YFP expression was first monitored for cells in exponential and stationary cultures under shaken or stagnant conditions (Figure 5A, B). Both exponential (Figure 5A) and stationary (Figure 5B) phase cultures show similar trends over a 32 h period. Shaken culture in induction medium (Figure 5A, B blue points), lead to significant expression of YFP over cells cultured in control medium (Figure 5A, B red points). However, the rate of YFP expression was much greater for *S. cerevisiae* in exponential vs stationary culture. Development of a fluorescence signal 3σ above the background fluorescence signal (LOD_{Fluor}, see the Experimental Section) in the shaken stationary phase culture required nearly 4.5 h. This signal took less than 2 h to develop in the shaken exponential phase culture. Although the saturation intensity (25 and 32 h time points) for

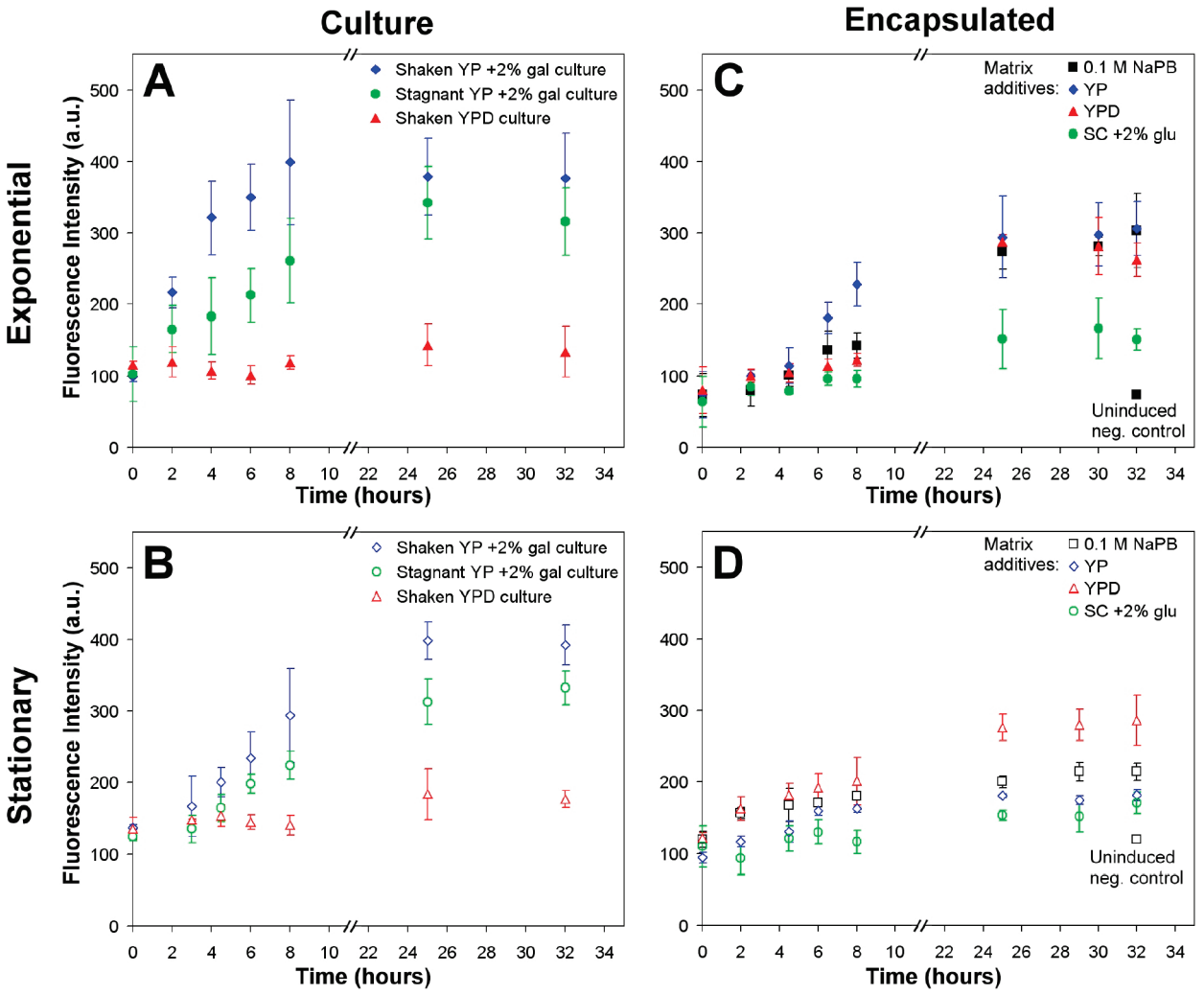

Figure 5. Rate of induced gene expression measured by YFP reporter protein fluorescence intensity for *S. cerevisiae* cells (A, B) under differing culture conditions and (C, D) encapsulated with in glycerol-silica matrixes with various additives. (A, C) Cells from exponential phase culture are shown with solid symbols; (B, D) stationary phase culture are shown with open symbols. *S. cerevisiae* cells encapsulated in glycerol−silica matrixes derived from 50 vol % PGS and 50 vol % medium that was: nutrient- and fermentable-carbon-rich (YPD, red), nutrient-rich without fermentable carbon (YP, blue), nutrient-restricted and fermentable-carbon-rich (SC +2% glu), or without nutrients or fermentable carbon (0.1 M NaPB, black). All media were adjusted to pH 6.0. Encapsulated *S. cerevisiae* cells from exponential culture were entrapped for 24−48 h, and cells from stationary culture were entrapped for 7 days prior to inducing gene expression. Encapsulated cells were stored at room temperature. Error bars in A and B are one standard deviation of measurements from 3 samples. Error bars in C and D are one standard deviation of measurements from 3 regions of a given sample. For clarity, only the final data point for uninduced negative control samples (YPD-treated) are shown in C and D. All negative control data points are presented in the Supporting Information, Figure S6.

both stationary and exponential phase cultures was similar, the initial background fluorescence for cells in stationary culture was higher (avg. 132 ± 6 au) than in exponential culture (avg. 105 ± 22 au), indicative of greater leaky expression for this construct in stationary phase culture. This higher background fluorescence also contributed to the delayed development of a signal greater than the LOD_{Fluor}. Finally, stagnant culture in induction medium (Figure 5A, B green points) showed a significantly lower rate of YFP expression and lower saturation intensity for both exponential and stationary phase *S. cerevisiae* cultures. This is attributed to the lower diffusion rate of the inducer molecule and oxygen required for fluorescence through the stagnant medium to the settled cells.

The rate of inducible gene expression of cells from exponential culture encapsulated in PGS derived silica gels with various media additives is presented in Figure 5C. Treatment with YP +gal induction medium on top of each of the encapsulated cell monoliths resulted in expression of YFP to varying degrees. Cells from exponential culture encapsulated with nutrient rich YP medium without fermentable carbon (Figure 5C, blue points) had the highest rate of gene expression, with a signal above the LOD_{Fluor} near 6.5 h from induction. This high rate relative to the other media additive samples may be due to the presence of some nutrients sustaining the metabolically active cells over the first 24−48 h of encapsulation, while not presenting a competing fermentable carbon source to the cells. In cultures with multiple fermentable carbon sources, yeast selectively metabolizes the most metabolically accessible carbon source, glucose.[50] This preferential metabolism of glucose could delay uptake and response to galactose, as was observed with YPD entrapped samples (Figure 5C, red points), which generated a signal above the

dx.doi.org/10.1021/cm103525u |*Chem. Mater.* 2011, 23, 2555–2564

LOD_{Fluor} after approximately 12 h, and with SC + 2% glu entrapped samples (Figure 5C, green points) which did not reach a signal above the LOD_{Fluor} over the course of the experiment. In addition to selective carbon uptake, the SC + 2% glu entrapped samples may have also suffered from low viability and locally high acidity from acetic acid generation. Cells entrapped with 0.1 M NaPB (Figure 5C, black points) showed a slightly higher rate of gene expression than the YPD samples (fluorescence intensity > LOD_{Fluor} at 10 h), which is again attributed to the lack of a competing carbon source. Among these 4 media, YP, NaPB, and YPD all reached a similar saturation level of fluorescence intensity (~290 au) 25 h after treatment with induction medium. This saturation level is very similar to that obtained for stagnate culture of exponential phase cells (Figure 5A, green points), and is also attributed to decreased diffusion of galactose and oxygen through the silica matrix.

Encapsulated cells from stationary culture also exhibited measurable YFP expression, as shown in Figure 5D, but at much lower rates than observed for cells from exponential culture. Similar to the higher background fluorescence observed between stationary and exponential phase cultures (Figure 5A, B), these samples exhibited higher background fluorescence (avg. 111 ± 13 au) in comparison to encapsulated cells from exponential culture (avg. 73 ± 7 au). Initially, rates between the mediums were similar (excluding SC +2% glu, for reasons already addressed). The development of a fluorescence intensity > LOD_{Fluor} for YP, YPD, and 0.1 M NaPB, took approximately 6, 5, and 8 h, respectively. Again, *S. cerevisiae* entrapped with SC + 2% glu did not reach a signal > LOD_{Fluor} after the 32 h treatment with inducer. At saturation, however, there was greater variation between cells entrapped in the various additives, with *S. cerevisiae* entrapped with YPD showing the highest fluorescence intensity, followed by NaPB and YP. YFP fluorescence intensity for cells entrapped in SC + 2% glu was measurable, but poor.

Ramifications for Encapsulated Living Cell-Based Biosensor Design. The results of this study provide key parameters for selection of cell metabolic phase and silica matrix additives for case-specific cell-based biosensing applications. For example, in the case of "leave behind" environment monitoring sensors, long-term viability is required. Quiescent cells should be selected and encapsulated without media to prevent exit from stationary phase. Such sensors could potentially operate for over 2 months under the conditions tested in this study, after which the sensors can be collected, analyzed, and replaced. The lower rate of gene expression for cells from stationary culture entrapped with buffer may not be a significant disadvantage as fast response time is often not a requirement. For online process monitoring, fast response times are required, therefore cells from exponential culture should be used to meet this requirement. The choice of media additives to the matrix is not as crucial, with the caveats that matrix additives should not compete with the target analyte, nor yield undesirable byproducts. Further, the low viability of cells from exponential culture would require weekly replacement of the sensor. Although not ideal, long-term viability is not a key requirement for online process monitoring which typically occurs in developed regions where replacement sensors can be stored under refrigeration, or received through reliable shipments.

CONCLUSIONS

Our investigations have shown the importance of the initial metabolic phase for encapsulated *S. cerevisiae* cells, and the presence of media additives to the encapsulation matrix, on the rate of reporter gene expression and long-term viability of the cells. Encapsulated cells from exponential cultures showed moderately higher rates of induced reporter gene expression, and quiescent cells exhibited significantly greater long-term viability. Addition of media components to the glycerol-silica matrix, while beneficial to reporter gene expression under certain conditions, adversely impacted long-term viability in all cases studied. This was attributed to components of media inducing exit of the cells from the more robust quiescent state, and the metabolic production of toxic byproducts. These results elaborate further on other silica gel whole-cell encapsulation studies, and provide important insights that may facilitate design and development of effective cell-based biosensors for case-specific applications.

ASSOCIATED CONTENT

Supporting Information. Figures S1−S6 and Table S1, described in the text. This material is available free of charge via the Internet at http://pubs.acs.org.

AUTHOR INFORMATION

Corresponding Author

*C.J.B.: Telephone: (505) 272-7627; Fax: (505) 272-7304; Email: cjbrink@sandia.gov. S.M.B.: Telephone: (505) 844-5105; Fax: (505) 845-8161; Email: smbrozi@sandia.gov. D.R.W.: Telephone: (505) 844-6631; Fax: (505) 845-8161; Email: drwheel@sandia.gov

ACKNOWLEDGMENT

This work was funded by the Defense Treat Reduction Agency (DTRA) Chem. Bio. Basic Research Program grant B084467I, the DoE NNSA Office for Nonproliferation Research and Development (NA-22), and the Sandia Lab Directed Research and Development program. CJB acknowledges funding from the Air Force Office of Scientific Research grant FA 9550-10-1-0054, and the U.S. Department of Energy, Office of Science, Office of Basic Energy Sciences, Division of Materials Sciences and Engineering. Sandia National Laboratories is a multiprogram laboratory operated by Sandia Corporation, a wholly owned subsidiary of Lockheed Martin Company, for the U.S. Department of Energy's National Nuclear Security Administration under Contract DE-AC04-94AL85000.

REFERENCES

(1) Meunier, C. F.; Dandoy, P.; Su, B. L. *J. Colloid Interface Sci.* **2010**, *342*, 211–224.

(2) Yap, F. L.; Zhang, Y. *Biosens. Bioelectron.* **2007**, *22*, 775–788.

(3) Harper, J. C.; Khirpin, C. Y.; Carnes, E. C.; Ashley, C. E.; Lopez, D. M.; Savage, T.; Jones, H. D. T.; Davis, R. W.; Nunez, D. E.; Brinker, L. M.; Kaehr, B.; Brozik, S. M.; Brinker, C. J. *ACS Nano* **2010**, *4*, 5539–5550.

(4) Baca, H. K.; Ashley, C.; Carnes, E.; Lopez, D.; Flemming, J.; Dunphy, D.; Singh, S.; Chen, Z.; Liu, N. G.; Fan, H. Y.; Lopez, G. P.; Brozik, S. M.; Werner-Washburne, M.; Brinker, C. J. *Science* **2006**, *313*, 337–341.

(5) Dave, B. C.; Dunn, B.; Valentine, J. S.; Zink, J. I. *Anal. Chem.* **1994**, *66*, A1120–A1127.

(6) Bjerketorp, J.; Hakansson, S.; Belkin, S.; Jansson, J. K. *Curr. Opin. Biotechnol.* **2006**, *17*, 43–49.

(7) Coradin, T.; Livage, J. *Acc. Chem. Res.* **2007**, *40*, 819–826.
(8) Stevens, M. M.; George, J. H. *Science* **2005**, *310*, 1135–1138.
(9) Zhang, S. G. *Nat. Biotechnol.* **2004**, *22*, 151–152.
(10) Carnes, E. C.; Lopez, D. M.; Donegan, N. P.; Cheung, A.; Gresham, H.; Timmins, G. S.; Brinker, C. J. *Nat. Chem. Biol.* **2010**, *6*, 41–45.
(11) Carnes, E. C.; Harper, J. C.; Ashley, C. E.; Lopez, D. M.; Brinker, L. M.; Liu, J. W.; Singh, S.; Brozik, S. M.; Brinker, C. J. *J. Am. Chem. Soc.* **2009**, *131*, 14255–14257.
(12) Raghavan, S.; Chen, C. S. *Adv. Mater.* **2004**, *16*, 1303–1313.
(13) Kandimalla, V. B.; Tripathi, V. S.; Ju, H. X. *Crit. Rev. Anal. Chem.* **2006**, *36*, 73–106.
(14) Carturan, G.; Dal Toso, R.; Boninsegna, S.; Dal Monte, R. *J. Mater. Chem.* **2004**, *14*, 2087–2098.
(15) Meunier, C. F.; Rooke, J. C.; Leonard, A.; Xie, H.; Su, B. L. *Chem. Commun.* **2010**, *46*, 3843–3859.
(16) Gupta, R.; Chaudhury, N. K. *Biosens. Bioelectron.* **2007**, *22*, 2387–2399.
(17) Avnir, D.; Coradin, T.; Lev, O.; Livage, J. *J. Mater. Chem.* **2006**, *16*, 1013–1030.
(18) Dunphy, D. R.; Alam, T. M.; Tate, M. P.; Hillhouse, H. W.; Smarsly, B.; Collord, A. D.; Carnes, E.; Baca, H. K.; Kohn, R.; Sprung, M.; Wang, J.; Brinker, C. J. *Langmuir* **2009**, *25*, 9500–9509.
(19) Hamm, C. E.; Merkel, R.; Springer, O.; Jurkojc, P.; Maier, C.; Prechtel, K.; Smetacek, V. *Nature* **2003**, *421*, 841–843.
(20) Premkumar, J. R.; Lev, O.; Rosen, R.; Belkin, S. *Adv. Mater.* **2001**, *13*, 1773–1775.
(21) Premkumar, J. R.; Rosen, R.; Belkin, S.; Lev, O. *Anal. Chim. Acta* **2002**, *462*, 11–23.
(22) Premkumar, J. R.; Sagi, E.; Rozen, R.; Belkin, S.; Modestov, A. D.; Lev, O. *Chem. Mater.* **2002**, *14*, 2676–2686.
(23) Sagi, E.; Hever, N.; Rosen, R.; Bartolome, A. J.; Premkumar, J. R.; Ulber, R.; Lev, O.; Scheper, T.; Belkin, S. *Sens. Actuators, B* **2003**, *90*, 2–8.
(24) Jia, J. B.; Tang, M. Y.; Chen, X.; Li, Q.; Dong, S. J. *Biosens. Bioelectron.* **2003**, *18*, 1023–1029.
(25) Trogl, J.; Ripp, S.; Kuncova, G.; Sayler, G. S.; Churava, A.; Parik, P.; Demnerova, K.; Halova, J.; Kubicova, L. *Sens. Actuators, B* **2005**, *107*, 98–103.
(26) Nguyen-Ngoc, H.; Tran-Minh, C. *Anal. Chim. Acta* **2007**, *583*, 161–165.
(27) Yu, D.; Volponi, J.; Chhabra, S.; Brinker, C. J.; Mulchandani, A.; Singh, A. K. *Biosens. Bioelectron.* **2005**, *20*, 1433–1437.
(28) Ferrer, M. L.; Yuste, L.; Rojo, F.; del Monte, F. *Chem. Mater.* **2003**, *15*, 3614–3618.
(29) Perullini, M.; Jobbagy, M.; Moretti, M. B.; Garcia, S. C.; Bilmes, S. A. *Chem. Mater.* **2008**, *20*, 3015–3021.
(30) Kuncova, G.; Podrazky, O.; Ripp, S.; Trogl, J.; Sayler, G. S.; Demnerova, K.; Vankova, R. *J. Sol—Gel Sci. Technol.* **2004**, *31*, 335–342.
(31) Ferrer, M. L.; Garcia-Carvajal, Z. Y.; Yuste, L.; Rojo, F.; del Monte, F. *Chem. Mater.* **2006**, *18*, 1458–1463.
(32) Allen, C.; Buttner, S.; Aragon, A. D.; Thomas, J. A.; Meirelles, O.; Jaetao, J. E.; Benn, D.; Ruby, S. W.; Veenhuis, M.; Madeo, F.; Werner-Washburne, M. *J. Cell Biol.* **2006**, *174*, 89–100.
(33) Khonina, T.; Chupakhin, O.; Larionov, L.; Boyakovskaya, T.; Suvorov, A.; Shadrina, E. *Pharm. Chem. J.* **2008**, *42*, 609–613.
(34) Brandhuber, D.; Torma, V.; Raab, C.; Peterlik, H.; Kulak, A.; Husing, N. *Chem. Mater.* **2005**, *17*, 4262–4271.
(35) Gill, I. *Chem. Mater.* **2001**, *13*, 3404–3421.
(36) Gill, I.; Ballesteros, A. *J. Am. Chem. Soc.* **1998**, *120*, 8587–8598.
(37) Nassif, N.; Bouvet, O.; Rager, M. N.; Roux, C.; Coradin, T.; Livage, J. *Nat. Mater.* **2002**, *1*, 42–44.
(38) Nassif, N.; Roux, C.; Coradin, T.; Rager, M. N.; Bouvet, O. M. M.; Livage, J. *J. Mater. Chem.* **2003**, *13*, 203–208.
(39) Fu, D.; Libson, A.; Miercke, L. J.; Weitzman, C.; Nollert, P.; Krucinski, J.; Stroud, R. M. *Science* **2000**, *290*, 481–486.
(40) Sahai, N.; Tossell, J. A. *Inorg. Chem.* **2002**, *41*, 748–756.
(41) Kemmitt, T.; Milestone, N. *Aust. J. Chem.* **1995**, *48*, 93–102.
(42) (a) Goldberg, E. P.; Powers, E. J. *J. Polym. Sci. Polym. Phys. Ed.* **1964**, *2*, 835.(b) Goneberg, A.; Verheyden, A. Belgian Patent 510419 (to Union chimique belge Soc.), 1952. (c) Krimm, H.; Schnell, H. German Patent 1136114 (to Farbenfabrik Bayer), 1962. (d) Vaughn, H. A. British Patent 989379, (to General Electric Co.), 1965.
(43) Brinker, C. J.; Scherer, G. W. *Sol—Gel Science*; Academic Press: New York, 1989.
(44) Brook, M. A.; Chen, Y.; Guo, K.; Zhang, Z.; Jin, W.; Deisingh, A.; Cruz-Aguado, J.; Brennan, J. D. *J. Sol—Gel Sci. Technol.* **2004**, *31*, 343–348.
(45) Gray, J. V.; Petsko, G. A.; Johnston, G. C.; Ringe, D.; Singer, R. A.; Werner-Washburne, M. *Microbiol. Mol. Biol. Rev.* **2004**, *68*, 187–206.
(46) Granot, D.; Snyder, M. *Proc. Natl. Acad. Sci. U.S.A.* **1991**, *88*, 5724–5728.
(47) Burtner, C. R.; Murakami, C. J.; Kennedy, B. K.; Kaeberlein, M. *Cell Cycle* **2009**, *8*, 1256–1270.
(48) Nassif, N.; Roux, C.; Coradin, T.; Bouvet, O. M. M.; Livage, J. *J. Mater. Chem.* **2004**, *14*, 2264–2268.
(49) van der Meer, J. R.; Belkin, S. *Nat. Rev. Microbiol.* **2010**, *8*, 511–522.
(50) Gelade, R.; Van de Velde, S.; Van Dijck, P.; Thevelein, J. *Genome Biol.* **2003**, *4*, 233.